PHYSICAL REVIEW D VOLUME 32, NUMBER 11 1 DECEMBER 1985

Measurement of D^0 lifetime in e^+e^- annihilation at high energy

H. Yamamoto,[α] W. B. Atwood,[β] P. H. Baillon,[β,(a)] B. C. Barish,[α] G. R. Bonneaud,[β] A. Courau,[β] G. J. Donaldson,[β,(b)] R. Dubois,[β,(c)] M. M. Duro,[β] E. E. Elsen,[β,(d)] S. G. Gao,[β,(e)] Y. Z. Huang,[α,(f)] G. M. Irwin,[β] R. Johnson,[β] H. Kichimi,[β,(g)] J. Kirkby,[β,(a)] D. E. Klem,[β] D. E. Koop,[α,(h)] J. Ludwig,[α,(i)] G. B. Mills,[α] A. Ogawa,[β] T. Pal,[α] D. Perret-Gallix,[β,(j)] R. Pitthan,[β] D. L. Pollard,[β,(k)] C. Y. Prescott,[β] L. Z. Rivkin,[α] L. S. Rochester,[β] W. Ruckstuhl,[α,(l)] M. Sakuda,[α] S. Sherman,[α,(m)] E. J. Siskind,[α,(n)] R. Stroynowski,[α] S. Q. Wang,[β,(f)] S. G. Wojcicki,[β] W. G. Yan,[β,(f)] and C. C. Young[β]

[α]*California Institute of Technology, Pasadena, California 91125*

[β]*Stanford Linear Accelerator Center and Physics Department, Stanford University, Stanford, California 94305*

(DELCO Collaboration)

(Received 3 June 1985)

A measurement of the D^0 lifetime using the impact-parameter method is presented. The D^0 sample is obtained from identified $D^{*\pm}$ decays in e^+e^- annihilations into hadrons at center-of-mass energy of 29 GeV. The maximum-likelihood method used is found to be insensitive to the specific choice of cuts and uncertainties in backgrounds, giving the D^0 lifetime of $[4.6\pm1.5$ (statistical)$^{+0.6}_{-0.5}$(systematic)$]\times10^{-13}$ sec. The consistency and bias of the method are checked. Combining the measurement with the semileptonic branching ratio of D^0, we estimate the semileptonic decay rate of D^0 to be $(1.6\pm0.6)\times10^{11}$ sec^{-1}. The corresponding value of the effective charm-quark mass is found to be consistent with the typical constituent mass of charm quark.

I. INTRODUCTION

Charmed mesons continue to provide us with many puzzles as well as clues to the structure and decay mechanism of hadrons. Among the most intriguing is the difference in the lifetime[1] and semileptonic branching fraction[2,3] of D^0 and D^+ mesons. If the charm quark decays independently of the light valence quark (spectator model) then the lifetime and the semileptonic branching fraction should be identical for both mesons. Two types of attempts have been made to accommodate the difference in the framework of the standard model. One is to enhance the nonleptonic decays of D^0, and the other is to suppress the nonleptonic decays of D^+.[4] In both approaches, the light quark plays an important role (nonspectator models) in the nonleptonic decays. The semileptonic decay rate, however, is expected to be the same for both mesons at least up to the Cabibbo suppression.[5-7] The lifetimes and the semileptonic branching fractions of D^0 and D^+ together give absolute measurements of their semileptonic decay rates, which can be compared with the theoretical predictions.

The lifetime of D^0 has been measured in various environments[1] including the e^+e^- annihilation,[8] where the crossing point of the two tracks from each D^0 decay is measured with respect to the center of the e^+e^- beams. In this report, we will describe a measurement of the D^0 lifetime with the DELCO detector at the SLAC e^+e^- storage ring PEP. The lifetime is obtained by a maximum-likelihood method using the impact parameters of individual tracks of D^0 decays.

II. PROCEDURE

The D^0 candidates are selected in the decays of charged D^*'s

$$D^{*+}\to D^0\pi^+_{D^*},\quad D^0\to K^-\pi^+(X) \tag{2.1}$$

(and its charge conjugate), where X, which is not observed, is typically a π^0, and the subscript D^* of the first pion is to distinguish it from the pion in the D^0 decay. For each of two charged tracks from the D^0 decay, the impact parameter b is defined in the plane perpendicular to the beam axis (xy plane) and with respect to the beam center measured by the beam-position monitor (Fig. 1). The sign of b is positive if the inner product of the D^0 momentum in the xy plane, $\mathbf{P}_{\perp D^0}$, and the vector from the beam center to the point of closest approach on the track, $\mathbf{b}$, is positive, and the sign is negative if the inner product is negative. The two cases are shown in Fig. 1.

If a D^0 is created at the beam center given by the beam-position monitor, and if the track is measured without errors, then the impact parameter b is always positive and given by $d_\perp\sin\theta$, where $d_\perp$ is the decay distance of D^0 projected onto the xy plane, and θ is the angle between $\mathbf{P}_{\perp D^0}$ and the track direction in the xy plane.

The true impact-parameter distribution is smeared because of the measurement errors and because the true primary vertex is only approximated by the beam center given by the beam-position monitor. As shown in detail in later sections, these errors can be well approximated by a Gaussian plus a flat background, where the width of the

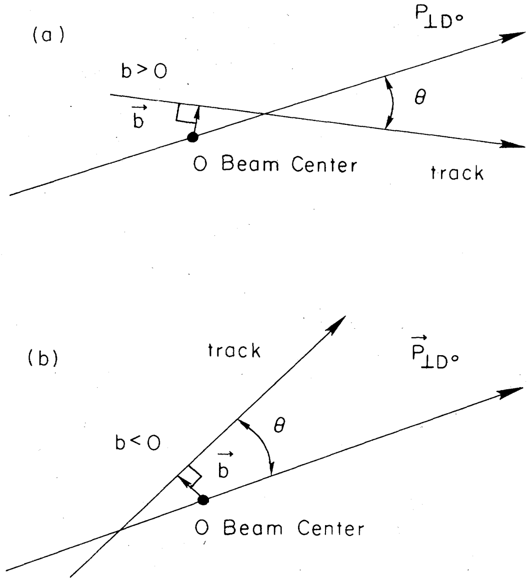

FIG. 1. The definition of the impact parameter and its sign. All parameters are defined in the plane perpendicular to the beam axis. The point 0 is the beam center given by the beam-position monitor. The impact parameter b is defined as $|\mathbf{b}|$ with the sign of $\mathbf{b}\cdot\mathbf{P}_{\perp D^0}$. The cases for positive and negative b are shown in (a) and (b), respectively.

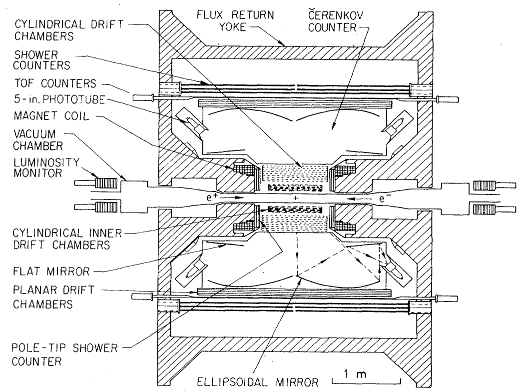

FIG. 2. The side view of the DELCO detector.

Gaussian depends on the configuration of each track. The probability that a track is not from a D^0 decay also varies from track to track.

In order to extract the D^0 lifetime from the impact parameters, we have chosen to employ a maximum-likelihood method which allows us to make the most out of the information available. In the following sections, we will discuss the components of the analysis.

III. COMPONENTS OF ANALYSIS

A. Detector

The side view of the DELCO detector is shown in Fig. 2. One of the unique features of the detector is the good particle-identification capability provided by its gas threshold Čerenkov counter.[9] The data used for this analysis was taken with isobutane gas as the Čerenkov radiator, which has thresholds at 2.6 GeV/c for a pion and at 9.2 GeV/c for a kaon. The counter consists of 36 cells covering 62% of 4π. Each cell is viewed by a RCA 8854 quantacon phototube coated with paraterphenyl to enhance the light collection in the UV region. For a Bhabha track, the average number of photoelectron is 18.

The Čerenkov counter is sandwiched by inner and outer drift chambers. The inner chambers consist of 6 layers (*uuzzvv*) of inner drift chamber (IDC) and 10 layers (*zzuuzzvvzz*) of central drift chamber (CDC). In the parentheses above, z indicates a layer with wires parallel to the beam axis, and u and v indicate layers with small-angle stereo wires (about ± 2 degrees). The innermost layer of the IDC is at $r = 12.0$ cm, and the outermost layer of the CDC is at 48.9 cm. The single-hit position resolution for a Bhabha track is 140 μm for the IDC and 200 μm for the CDC. It leads to the impact-parameter resolution of 230 μm without fixing the momentum of Bhabha tracks to the beam energy. The outer drift chambers are made of 6 modules of planar chambers that form a hexagon. Each module contains 6 layers (*zzuvzz*), where u and v are large-angle (± 30 degrees) stereo layers. The single-hit resolution of the outer chambers is 450 μm. The magnet is of the Helmholtz type in order to reduce the amount of material before the Čerenkov counter. The field is 3.3 kG at the center and the total $\int B\,dl$ is 1.8 kG m. The resulting momentum resolution is $\sigma_P/P = [(2\% P)^2 + (6\%)^2]^{1/2}$ where P is in GeV/c. The data correspond to an integrated luminosity of 150 pb^{-1}.

B. Beam-position monitor

The beam-position monitors are located ± 3.74 m from the interaction point. Each consists of four electrodes (buttons) placed inside the vacuum pipe which pick up pulses generated by the passing beam bunches. A total of eight pulse heights from the buttons are recorded for the bunch corresponding to each event and from these the beam centroid position at the interaction region is calculated event by event.

In Fig. 3, the interaction points of Bhabha events are compared with the beam center measured by the beam-position monitor. For a Bhabha track emitted almost vertically (within ± 0.25 rad in ϕ), the x coordinate of the vertex is well approximated by the x coordinate of the origin of the track. The y coordinate is obtained similarly using the tracks emitted almost horizontally (within ± 0.20 rad). Figures 3(a) and 3(c) show the x-coordinate values in the laboratory frame and relative to the beam-position-monitor value, respectively. Figures 3(b) and 3(d) show the same for the y coordinate. Even though the fluctuation of the beam position is as large as 3 mm, it can be seen that the beam-position monitor is tracking the true beam center reasonably well.

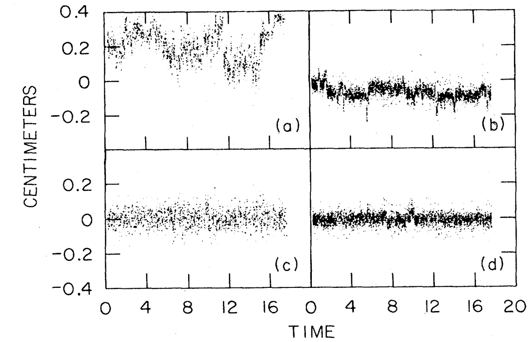

FIG. 3. The x coordinate of the interaction points of Bhabha events, in the detector frame (a), and relative to the beam position given by the beam-position monitor (c). The horizontal axis is the time in an arbitrary unit. The same set of figures for the y coordinate is given in (b) and (d). The time range shown corresponds to data set 2, which accounts for about one-half of the whole data.

C. Beam sizes

There are three data blocks 1, 2, and 3 with different configurations. The tracking qualities are roughly the same for the three.

The beam cross section is approximated by a two-dimensional Gaussian with widths σ_x and σ_y. Then the error in the impact parameter due to the beam size at an azimuthal angle ϕ is given by

$$\sigma_{\text{beam}}(\phi)^2=\sigma_x{}^2\cos^2\phi+\sigma_y{}^2\sin^2\phi \ . \tag{3.1}$$

The beam size is obtained by measuring the width of the impact-parameter distribution of Bhabha tracks and then subtracting the measurement error in quadrature. The measurement error is estimated by the width of the distribution of the track separation near the beam. Figure 4 shows the measured $\sigma_{\text{beam}}{}^2$ as a function of ϕ for data set 2. The smooth curve is a fit to the expected shape (3.1) with σ_x and σ_y as parameters. The results are summarized in Table I for the three data sets. The values calculated from the machine parameters of the storage ring[10] are also listed. The calculation ignores nonlinear and incoherent effects such as beam-beam interactions, which

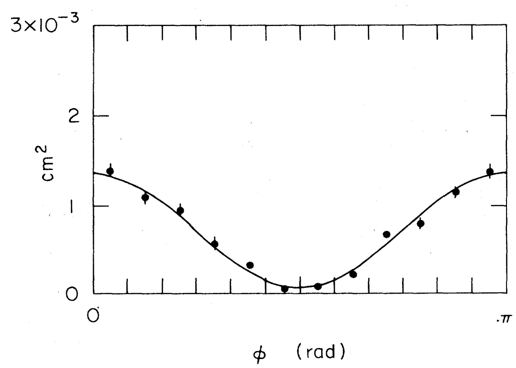

FIG. 4. The beam variance vs ϕ (data set 2). The measurement errors have been already subtracted. The solid curve is the result of the fit of the shape $\sigma_x{}^2\cos^2\phi+\phi_y{}^2\sin^2\phi$.

TABLE I. Beam sizes obtained from Bhabha tracks and those expected from the machine parameters of the storage ring. Values are shown separately for the three data sets.

(μm)		1	2	3
Measured	σ_x	462 ± 6	369 ± 6	342 ± 4
	σ_y	113 ± 10	75 ± 17	83 ± 12
Expected	σ_x	380	420	420
	σ_y	$\lesssim100$	$\lesssim100$	$\lesssim100$

probably is the source of the discrepancy between the measured and expected values. It is worth noting that the measured beam sizes are the true sizes convoluted with the resolution of the beam-position monitor, which are what we need for the fit of D^0 lifetime, since the D^0 tracks are also measured with respect to the beam position given by the beam-position monitor.

D. Measurement error in hadronic events

There are three contributions to the impact parameter error σ

$$\sigma^2=\sigma_{\text{beam}}{}^2+\sigma_{\text{m.s.}}{}^2+\sigma_{\text{trk}}{}^2 \ , \tag{3.2}$$

where σ_{beam} is given by (3.1), $\sigma_{\text{m.s.}}$ is due to the multiple scattering at the beam pipe and the inner wall of IDC, and σ_{trk} is due to tracking errors inside the drift chambers.

We use the following formula[11] for $\sigma_{\text{m.s.}}$:

$$\sigma_{\text{m.s.}}=\frac{r_{\text{eff}}}{\cos\lambda}\frac{0.0141}{P\beta}\left[\frac{X}{\cos\lambda}\right]^{1/2}\left[1+\frac{1}{9}\log_{10}\frac{X}{\cos\lambda}\right] , \tag{3.3}$$

where r_{eff} is the effective average radius of the materials before the tracking volume, which is 9.1 cm for data sets 1 and 2, and 9.0 cm for data set 3; λ is the angle of the track away from the plane perpendicular to the beam axis; P,β are the momentum (in GeV/c) and the velocity of the particle; and X is the total amount of material in the direction perpendicular to the beam axis (in radiation length), which is 2.25% for data sets 1 and 2 and 1.28% for data set 3.

This formula is good to a few percent in the cases of interest. There are, however, non-Gaussian components due to plural and single scatterings. They will be treated as part of the flat background.

The error σ_{trk} includes the measurement error of each drift-chamber hit, the effect of taking wrong hits (i.e., the partial confusion in tracking), and the effect of multiple scattering inside the tracking volume due to the gas, wires, and other materials along a track. The track-fitting program returns an estimated error for the impact parameter, σ_{fit}, assuming that all the points associated with the track are correct and the measurement error of each point is properly estimated. Even though it is a useful indication of the quality of the measured impact parameter, a correction has to be made to obtain a realistic σ_{trk} in actual hadronic events.

In order to obtain the functional form of the correction,

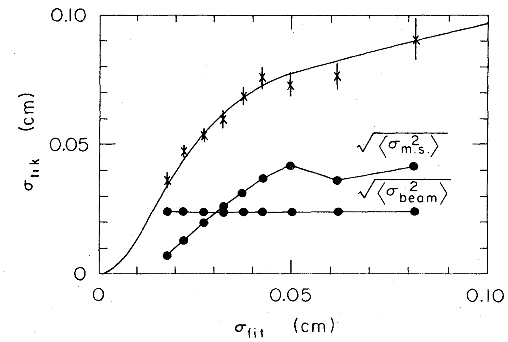

FIG. 5. The error due to the tracking σ_{trk} is plotted against the error given by the track-fitting program, σ_{fit}. The solid curve is a function fitted to the data points. The broken lines show the root mean squares of $\sigma_{m.s.}$ and σ_{beam} in each bin.

general hadronic tracks are divided into σ_{fit} bins. In each bin the impact-parameter distribution[12] is fitted with a Gaussian plus a flat background. The flat background is expected from strange-particle decays, nuclear interactions, etc. In principle, the decay products of heavy hadrons can broaden the distribution. However, a Monte Carlo study has shown that the effect is negligible in estimating σ_{trk}.[13]

Also, the root mean squares of $\sigma_{m.s.}$ and σ_{beam} are calculated for the tracks in each σ_{fit} bin and are quadratically subtracted from the measured width to get σ_{trk}. Figure 5 shows the resulting σ_{trk} as a function of σ_{fit}. The broken lines show the root mean squares of $\sigma_{m.s.}$ and σ_{beam}, which have been subtracted in each bin. The curve is a fit to the correction function.

In Fig. 6, the impact-parameter distribution is shown for each σ bin, where σ is obtained by (3.2). The curve in each plot is the result of fit with a Gaussian plus a flat background, where the width of Gaussian is fixed to the expected value. The functional shape gives a good fit in all σ bins. Also, even though σ_{trk} is inferred in each σ_{fit} bin and not in each σ bin, the final expected resolution well matches the real resolution in each σ bin.

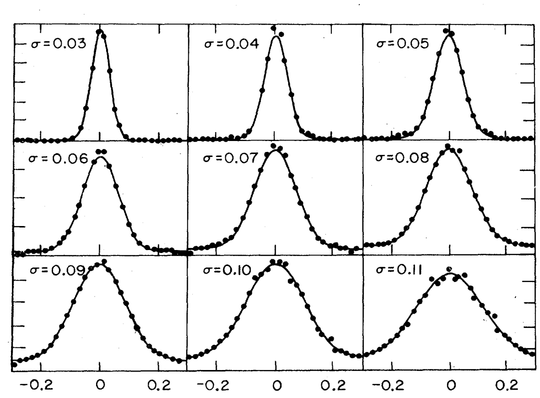

FIG. 6. The impact-parameter distribution is plotted for each bin of the overall expected error, σ. In each plot, the center value of σ is indicated in units of cm, and the curve is the result of fit with the expected Gaussian plus a flat background.

E. D^0 track selection

The D^0 tracks are selected as the decay products of charged D^*'s in the decay chain (2.1). The method takes advantage of the low-Q value of the D^* decay that limits the phase space thus suppressing the random background.[14] In this analysis, we further enhance the signal by using the Čerenkov counter to select the kaon or the pion from the D^0 decay.[15] Kaon candidates are selected by requiring tracks with P greater than 3.2 GeV/c to have no response in the associated Čerenkov cell. On the other hand, the criteria for pion candidates are $2.6 < P < 9$ GeV/c and that the associated Čerenkov cell has a response of more than 3 photoelectrons. These kaon and pion candidate tracks have substantial momenta, and are called "leading" tracks. Each of them is then combined with another track of the opposite sign (nonleading track) to form a D^0 candidate. When the leading track is a kaon (pion) candidate, we call it a K-mode (π-mode) combination. For a K-mode candidate, the kaon mass is assigned to the leading track and the pion mass is assigned to the nonleading track. For a π-mode candidate, the mass assignments are inverted accordingly. After the invariant-mass cut of $1.45 < M_{K\pi} < 2.2$ GeV/c^2, each D^0 candidate is combined with another track (π_{D^*} candidate) within the cone of $\sin\theta_{D^0\pi_{D^*}} < 0.13$. The π_{D^*} candidate track is said to be the "wrong" sign if its charge is the same as that of the track assigned the kaon mass, and the "right" sign if not. The mass difference $\Delta M = M_{K\pi\pi_{D^*}} - M_{K\pi}$ is plotted in Fig. 7 for both the K-mode and π-mode samples. The enhancement of the right-sign sample over the wrong-sign

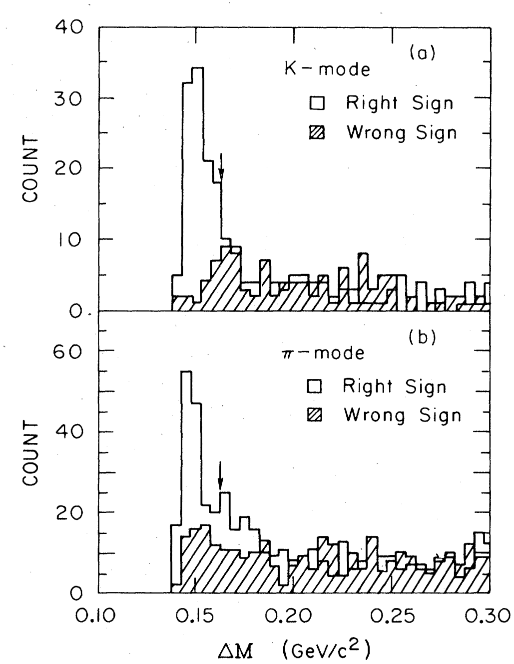

FIG. 7. The mass difference $\Delta M = M_{K\pi\pi_{D^*}} - M_{K\pi}$ for (a) the K mode, and (b) the π mode. The distributions for wrong-sign candidates (shaded) are plotted over those for right-sign candidates. The arrows show the position of ΔM cut.

sample is clear for both modes. The signal region is taken to be $\Delta M < 0.1625$ GeV/c^2.

We do not detect all the decay products of D^0 except in the $K^-\pi^+$ decay mode. Thus, when the $K\pi$ mass is measured lower than the nominal D^0 mass, the apparent D^* momentum is systematically shifted lower than the real value. In order to take this into account, the measured D^* momentum is corrected depending on the measured $K\pi$ mass. The correction is estimated by the Monte Carlo and is largest at the lower edge of the $K\pi$ mass range where the correction factor is 1.21. The overall D^0 momentum resolution is 9%, and the resolution of D^0 direction in the xy plane is 0.02 rad.

Without further cuts, there are 104 K-mode D^* candidates and 122 π-mode D^* candidates in the right-sign sample. There are 18 candidates overlapping the two modes which we have classified as K mode. The tracks of the wrong-sign candidates are not used in the lifetime fit except in the estimation of the non-D^0 background.

Then, the following cuts are made to the candidate tracks.

(1) P greater than 250 MeV/c. This is to reject tracks with a large error in impact parameter; it rejects 5 out of the 452 tracks.

(2) $\eta \sin\theta > 0.4$, where $\eta \equiv P_{\perp D^0}/M_{D^0}$ and θ is defined in Fig. 1. This is the ratio of the impact parameter to the decay distance of D^0 when errors are ignored. The larger this value is, the more weight the track has in the lifetime determination. And if it is zero, the track does not contribute to the lifetime measurement. Thus, even though this cut eliminates 173 out of 447 tracks, it does not degrade the statistical error of the fit while making it less sensitive to the background. Figure 8 shows the $\eta \sin\theta$ distributions for all the D^0 candidate tracks in the data. It can be seen that most of the tracks rejected are the leading tracks.

(3) $|b| < 2.5$ mm. This defines the window of impact parameter; it removes 5 more tracks, leaving 269.

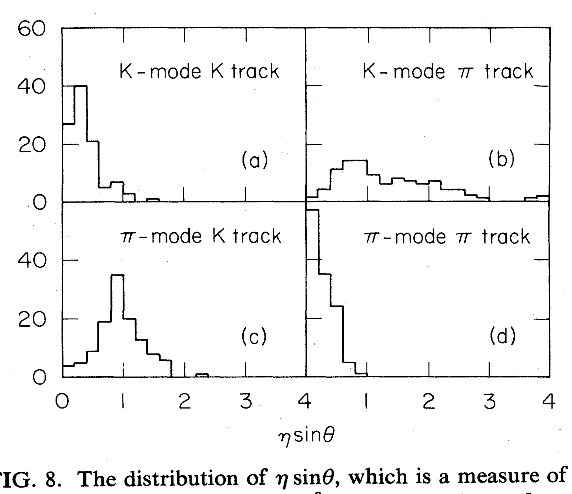

FIG. 8. The distribution of $\eta \sin\theta$, which is a measure of the sensitivity of each track to the D^0 lifetime, is shown for each track category in the D^0 sample. The leading tracks (K-mode K tracks, and π-mode π tracks) are less sensitive than the nonleading tracks.

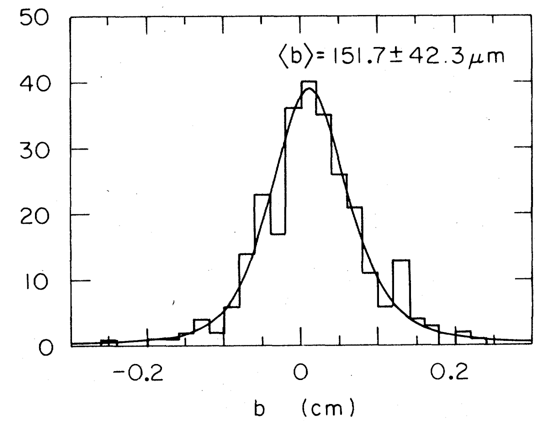

FIG. 9. The impact-parameter distribution for the final D^0 candidate tracks in the D^* sample. The solid curve is the result of the likelihood fit.

Figure 9 shows the impact-parameter distribution after the cuts. The distribution is clearly shifted in the positive direction, and the mean of the distribution is 151.7 ± 42.3 μm. The curve overplotted is the result of the fit described later.

Two different control samples are checked.

(a) General hadronic tracks with $P > 250$ MeV/c and $|b| < 2.5$ mm, where the thrust axis is used as the D^0 direction. The positive direction on the axis is defined such that the angle between the track and the axis is less than 90 degrees in the xy plane.

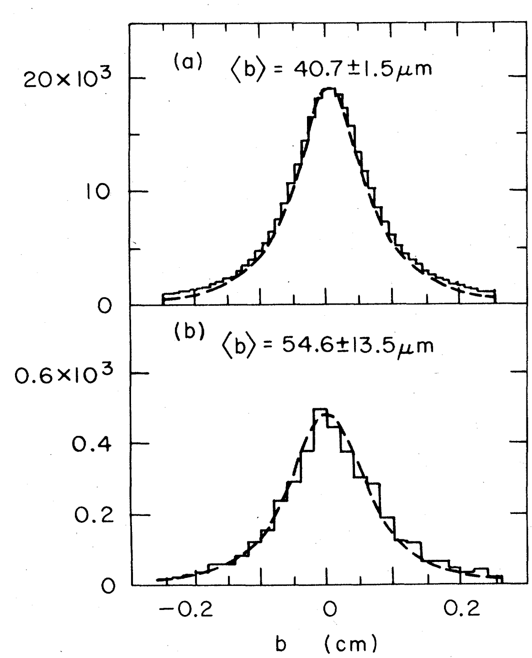

FIG. 10. The impact-parameter distributions for (a) the general tracks in hadronic events and (b) the tracks kinematically similar to the D^0 tracks. The corresponding distributions for the Monte Carlo simulation are overplotted (dashed curves).

TABLE II. The means of the impact parameter for the D^0 sample and the two control samples: (a) for the general hadronic tracks and (b) for the tracks kinematically similar to the D^0 candidate tracks.

$\langle b \rangle$ (μm)	Data	Monte Carlo
D^0 candidates	151.7 ± 42.3	
(a) General tracks	40.7 ± 1.5	34.9 ± 1.6
(b) Selected tracks	54.6 ± 13.5	43.4 ± 11.7

(b) The sample of tracks kinematically similar to the D^0 tracks. It is formed by taking all the D^0 candidates selected just as before but without the information of the Čerenkov counter and without combining them with π_{D^*} candidates.

The impact-parameter distributions for the two control samples are shown in Fig. 10, and the results are summarized in Table II. The corresponding shapes for the Monte Carlo simulation[16] are overplotted in Fig. 10 as dashed curves, and their mean values are also included in Table II. Positive mean values are expected because of strange- and heavy-particle decays, and the discrepancies between the data and the Monte Carlo simulation can be comfortably accommodated within the uncertainties in the production rates and the lifetimes of these particles (in particular bottomed hadrons).

The mean value of the impact parameter is not shifted by nuclear interactions, Coulomb scattering at the beam pipe region, γ conversions, or small misalignments of the drift chambers, etc. The changes in the measured impact parameter due to these sources are expected to be symmetric and do not alter the mean value.

F. Estimation of background

1. Non-D^0 tracks

To study non-D^0 background, we compare the right-sign and wrong-sign samples. The background in the D^* sample has the same amount of right-sign and wrong-sign combinations. Therefore, the number of right signs minus the number of wrong signs indicates the number of true D^*'s for which both the leading track and the π_{D^*} track are found correctly. However, the nonleading tracks populate the same momentum region as the average hadronic tracks and are more easily contaminated than the leading tracks are. Also, the Cabibbo-angle-suppressed decays of D^0 that generate a wrong-sign kaon contribute to the wrong-sign K-mode sample. In addition, when a D^0 decay contains multiple charged pions, a wrong-sign pion can become the leading pion candidate thus contributing to the wrong-sign π-mode sample even if the tracks are genuinely from a D^*. Therefore, the number of right signs minus wrong signs has to be multiplied by a correction factor to get the number of candidates for which the track of interest is correctly found. We assume the D^0-$\bar{D}^0$ mixing to be negligible.[15]

The correction factor r_{corr} is obtained by the Monte Carlo according to

$$r_{corr} = \frac{(\text{No. of correct tracks in the right-sign sample})}{(\text{No. of right signs}) - (\text{No. of wrong signs})} .$$

TABLE III. The fraction of the tracks from D^0 decays (purity) in each track category. The definition of the correction factor r_{corr} is given in the text.

		r_{corr}	Purity
K mode	K	1.09	$0.94 \pm 0.03 \pm 0.02$
	π	0.93	$0.80 \pm 0.03 \pm 0.04$
π mode	K	1.16	$0.67 \pm 0.07 \pm 0.07$
	π	1.48	$0.85 \pm 0.09 \pm 0.05$

Table III summarizes the result. The purity is defined to be the probability that the track is truly from a D^0 decay. The first errors in the purities are statistical and the second errors systematic. The systematic errors are due to the uncertainty in the correction factors. For the leading tracks, the uncertainty comes mostly from our imperfect knowledge on the decay branching fractions of D^0. The nonleading tracks have larger systematic errors corresponding to the added contamination.

2. D^*'s from b quarks

Since a decay of a b quark almost always creates a c quark,[17] we expect some of the D^*'s in our data set to come from the decays of b-flavored particles. The average $c\tau$ of the b hadrons is relatively long and of the order of several hundred microns,[18,19] which substantially changes the impact parameters of the D^0 tracks originating from b-flavored hadrons.

The number of D^0 tracks coming from b quarks is estimated by the Monte Carlo method using the same set of D^* selection and track cuts as for the data, where the

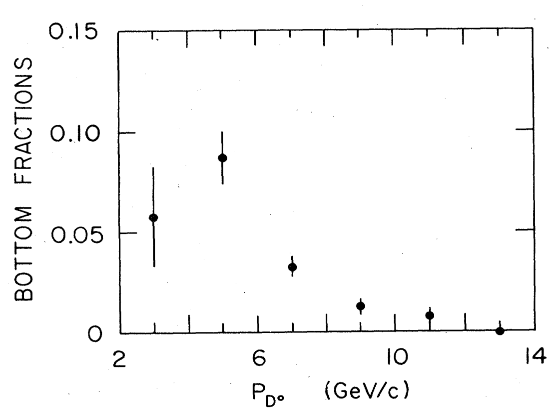

FIG. 11. The Monte Carlo estimated fraction of tracks that come from b-particle decays as a function of the D^0 momentum.

direct production ratio of D^* to D is set to 1 in the decays of b hadrons. The result is shown in Fig. 11 as a function of D^0 momentum P_{D^0}. The amount of contamination is similar for K tracks and π tracks, and the mean of the impact parameter for these tracks, κ_b, is found to be flat in $\eta \sin\theta$. With the average b lifetime of 350 μm (Ref. 19), and the D^0 lifetime of 136 μm, κ_b is estimated to be 210 μm. It does not depend strongly on the D^0 lifetime.

IV. LIKELIHOOD FIT OF D^0 LIFETIME

A. D^0 lifetime likelihood function

For N measurements of impact parameter b^i ($i=1,\ldots,N$), in which each event is characterized by a set of parameters $\mathbf{a}^i$, the likelihood function for $l \equiv c\tau$ is given by

$$L(l)=\prod_{i=1}^{N} f(b^i,l,\mathbf{a}^i) ,$$
$$f(b^i,l,\mathbf{a}^i)=\frac{f^0(b^i,l,\mathbf{a}^i)}{\int_{b_1}^{b_2} f^0(b,l,\mathbf{a}^i)db} , \tag{4.1}$$

where f and f^0 are the single-event likelihood function with and without the effect of the impact-parameter window, respectively, and (b_1,b_2) defines the window. The actual function to be minimized, $\mathcal{L}$, is defined by

$$\mathcal{L}(l) \equiv -2\ln L(l) = -2\sum_{i=1}^{N} \ln f(b^i,l,\mathbf{a}^i) . \tag{4.2}$$

The function f^0 is a convolution of an exponential with decay constant $\kappa = l\eta \sin\theta$ and a Gaussian with width σ, and can be written using the complementary error function,[20]

$$f^0(b,l,\mathbf{a}) \equiv f^0(b,\kappa,\sigma)$$
$$=\frac{1}{2\kappa}\exp\left[\frac{\sigma^2}{2\kappa^2}-\frac{b}{\kappa}\right]\operatorname{erfc}\left[\frac{1}{\sqrt{2}}\left[\frac{\sigma}{\kappa}-\frac{b}{\sigma}\right]\right] , \tag{4.3}$$

where f_0 is a function of l only through κ, and both κ and σ are functions of $\mathbf{a}$. The shape of f^0 as a function of b is shown in Fig. 12 for $\sigma = 500$ μm and several different κ's. The integration of f^0 needed in (4.1) is given by

$$\int_{b_1}^{b_2} f^0(b,\kappa,\sigma)db = \tfrac{1}{2}[e^{2\alpha x-\alpha^2}\operatorname{erfc}(x)+\operatorname{erf}(x-\alpha)]_{x_1}^{x_2} , \tag{4.4}$$

where

$$\alpha=\frac{\sigma}{\sqrt{2}\kappa},\quad x_k=\frac{1}{\sqrt{2}}\left[\frac{\sigma}{\kappa}-\frac{b_k}{\sigma}\right] \quad (k=1,2) . \tag{4.5}$$

The non-D^0 background is handled by adding a term which represents the distribution of the general background shape. We take it to be $\beta f^0(b,\kappa_B,\sigma)$, where β is the background fraction (1-purity) (see Table III), σ is the expected impact-parameter resolution for the track, and κ_B is a global constant that arises because the background does include genuinely positive impact parameters. We use a value $\kappa_B = 54.6$ μm from Fig. 10(b). Even though the true distribution is not exactly a convolution of an exponential and a Gaussian, this approximation is good enough, and the result is insensitive to the exact shape. The b-quark contamination is handled in the same way by adding $\delta f^0(b,\kappa_b,\sigma)$ to the likelihood function, where δ is the fraction of the tracks originating from b quarks and κ_b is the mean impact parameter for those tracks.

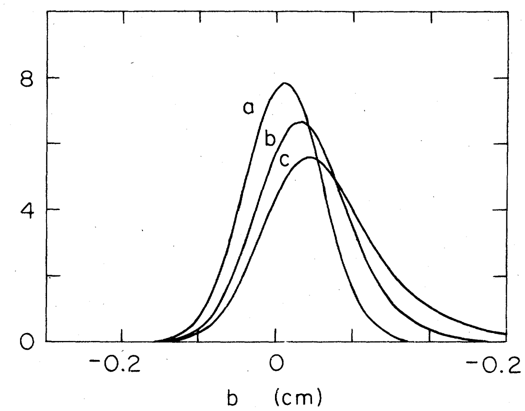

FIG. 12. The shape of $f^0(b,\kappa,\sigma)$ [formula (4.3)] is shown for $\sigma = 500$ μm (fixed) and $\kappa = 100$ (a), 400 (b), and 700 μm (c).

The flat background of the impact-parameter distribution cannot be reliably estimated *a priori* for the D^0 tracks from the general hadronic tracks because the sources of flat background are different for the two samples. Instead, we take the level of flat background, γ, to be the second parameter of the fit.

Putting everything together, our final properly normalized single-event likelihood function is

$$f(b,l,\mathbf{a}) = A[(1-\beta-\delta)f^0(b,\kappa,\sigma)$$
$$+\beta f^0(b,\kappa_B,\sigma)+\delta f^0(b,\kappa_b,\sigma)+\gamma] \tag{4.6}$$

with

$$A=\left[(1-\beta-\delta)\int_{b_1}^{b_2} f^0(b,\kappa,\sigma)db+\beta\int_{b_1}^{b_2} f^0(b,\kappa_B,\sigma)db\right.$$
$$\left.+\delta\int_{b_1}^{b_2} f^0(b,\kappa_b,\sigma)db+(b_2-b_1)\gamma\right]^{-1}$$

where f^0 is a function given by (4.3), and its integration is given by (4.4); $\kappa = l\eta\sin\theta$, with $\eta = P_{\perp D^0}/M_{D^0}$; σ is the overall error in the impact parameter, given by (3.2); β is the background fraction and given by Table III; κ_B is a constant (54.6 μm) that represents the positive mean impact parameter of the background; δ is the fraction of tracks that come from b quarks and given by Fig. 11; κ_b is the mean impact parameter of the D^0 tracks originating from hadrons containing b quarks (240 μm); and γ is a constant that represents the flat background, which is the second parameter of the fit.

The 1σ contour of the fit is shown in Fig. 13, and the results for the individual parameters are $c\tau = 136\pm46$ μm and $\gamma = 0.078^{+0.058}_{-0.042}$ cm^{-1}. The value of γ corresponds to a flat background of about 4% of the total area. The effect of the flat background is not large.

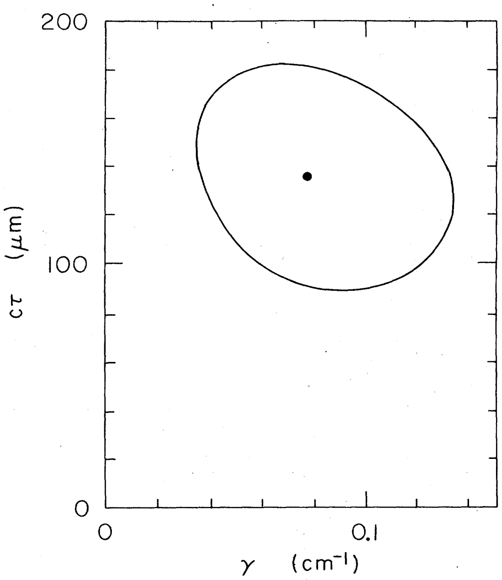

FIG. 13. 1σ contour of the likelihood fit. The two parameters are the level of the flat background, γ, and the D^0 lifetime $c\tau$. The result for $c\tau$ is 136±46 μm.

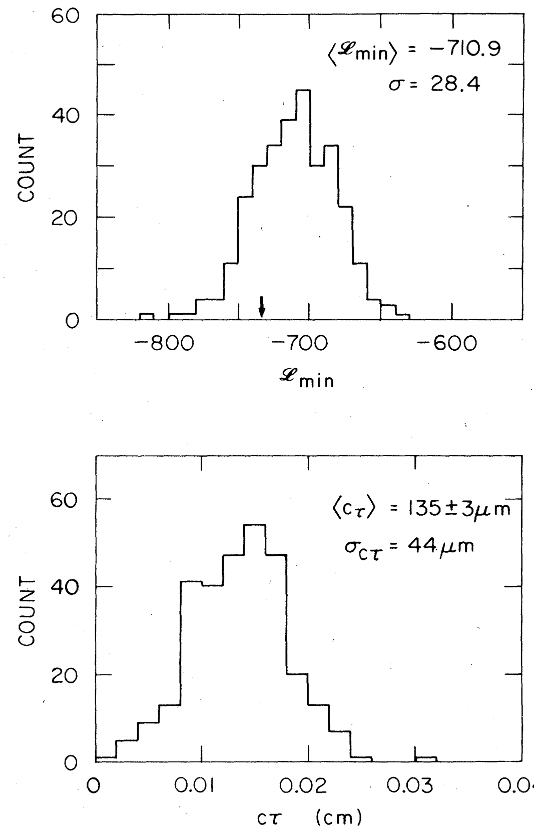

FIG. 14. (a) The simulated $\mathscr{L}_{min}$ using the measured $c\tau$ of 136 μm and the actual event configuration of each event in the data. The arrow indicates the $\mathscr{L}_{min}$ for the actual data. The distribution of $c\tau$ obtained at the same time is shown in (b).

B. Goodness of fit and bias check

One way to check the goodness of fit is to bin the impact parameters into a histogram and compare it to the expected shape from the result of the fit. The expected shape is given by

$$\left[\sum_{i=1}^{N} f(b,l^0,\mathbf{a}^i)\right]\Delta b \ ,$$

where f is given by the formula (4.6), Δb is the bin width of the histogram, and the lifetime l^0 is the result of the fit. The curve is overplotted in Fig. 9. The χ^2 of the fit is 8.9 for 10 degrees of freedom.[21]

Another way to check the fit, which is independent of the binning, makes use of the similarity between $\mathscr{L}$ and χ^2. The function $\mathscr{L}$ is equivalent to χ^2 up to a constant offset when the function f's are all Gaussian with each measurement representing a single data point of the χ^2 estimation. In the case of χ^2, the expected distribution of the minimum is a function of the number of degree of freedom and is well known. For $\mathscr{L}_{min}$, the expected distribution is not known *a priori*, but can be estimated by a simulation as follows. Using the result of the fit l^0, one impact parameter is generated for each track of the data according to the formula (4.6) using the same σ, κ's, etc., as used in the likelihood fit. Then, taking these impact parameters as input data, the likelihood analysis is repeated and $\mathscr{L}_{min}$ is calculated. The process is repeated from the beginning many times to generate the distribution of $\mathscr{L}_{min}$. If the fit is good, the measured $\mathscr{L}_{min}$ should be inside the central distribution. The result is shown in Fig. 14(a). The arrow indicates the observed value of $\mathscr{L}_{min}$. The goodness of the fit is reasonable with a 20% chance of getting a better $\mathscr{L}_{min}$ than the one observed.

As a by-product, the bias of the fit is checked by the distribution of $c\tau$ that corresponds to each of the simulated $\mathscr{L}_{min}$. It is shown in Fig. 14(b). The mean of the reconstructed $c\tau$'s agrees well with the input, namely, the method is biasfree within the statistical error. Also, the width of the distribution (44 μm) is in good agreement with the range of 1σ estimated by $\mathscr{L}-\mathscr{L}_{min}<1$, which is ±46 μm.

C. Systematic errors

1. Non-D^0 background (β,κ_B)

The systematic errors of the estimation of non-D^0 background in Table III are likely to have positive correlations, and have been added linearly. The statistical errors in Table III, on the other hand, are added quadratically. The combined error in $c\tau$ is found to be symmetric and ±4 μm. The other parameter related to the non-D^0 background is the mean of the impact parameters, κ_B, for those tracks. We used a value of 54.6 μm as determined from tracks kinematically similar to the D^0 candidates [Fig. 10(b)]. We estimate the error of κ_B to be ±15 μm which corresponds to ±3 μm in $c\tau$. The overall error from the non-D^0 background is then ±5 μm.

2. *Bottom contribution* (δ, κ_b)

The contribution from b quarks depends on the ratio $\Gamma(b \to c \to D)/\Gamma(b \to c \to D^*)$. In the Monte Carlo simulation, this was set to unity. When the ratio is varied between 4 to $\frac{1}{4}$, the resulting $c\tau$ changes at most ± 3 μm. The value of the average b-hadron lifetime, κ_b, also affects the result; we change the average b lifetime between 0.7 and 2.3×10^{-12} sec (Refs. 18 and 19) to get corresponding $c\tau$ errors of $^{+6}_{-7}$ μm. Since the above two systematics are not correlated, they are added in quadrature to give $^{+7}_{-8}$ μm.

3. *Mass assignments*

The mass assignment affects the lifetime through the multiple-scattering error $\sigma_{\text{m.s.}}$. The leading tracks are selected by the Čerenkov counter and the effect of the misidentification is negligible. Also, the nonleading tracks in the K mode can be safely assumed to be pions. However, the nonleading K tracks in the π mode are not all kaons. Even if we assume them to be all pions the resulting $c\tau$ increases by only 3 μm.

4. *Track momentum cut*

Removing the cut changes the result by less than 1 μm. Setting the cut at 750 MeV/c instead of 250 MeV/c removes 49 tracks, giving a lifetime of 134^{+51}_{-58} μm. Thus, there is no indication of bias from the track momentum cut.

5. *Impact-parameter window*

Our fit is relatively insensitive to the window because of the inclusion of the flat tail in the likelihood function. Changing the cut value in the range ± 0.5 mm around the standard value of 2.5 mm, the variation in $c\tau$ is found to be $^{+7}_{-4}$ μm.

6. *Expected impact-parameter error* (σ)

There are several factors that contribute to the expected error in the impact parameter as shown in (3.2). However, they are highly correlated in the sense that the result has to fit the impact-parameter distribution in the final data. The χ^2 of the expected impact-parameter distribution to the binned data increases at least one unit when the σ's are scaled by 0.9 and 1.1, which in turn translates to the error in $c\tau$ of $^{+14}_{-7}$ μm. The smaller the σ, the larger the lifetime.

7. $\eta \sin\theta$ *cut*

This cut removes the tracks that have little significance in the fit. Removing the cut brings in 173 tracks and the lifetime becomes 126 ± 45 μm. No significant improvement in the error is observed. We take the systematic error due to this cut to be $^{+0}_{-10}$ μm.

8. *Errors in* η *and* $\sin\theta$

The direction and the momentum of the D^0 are well determined. The resolutions of η and $\sin\theta$ are found to have negligible effect on the result.

The above items are expected to be independent of each other; thus, they are added quadratically. The items that have to be treated linearly have been already done so inside each category. The final overall systematic error in $c\tau$ is $^{+18}_{-16}$ μm.

V. SUMMARY AND DISCUSSION

We have measured the lifetime of D^0 meson using the impact parameters of D^0 tracks with respect to the beam center given by the beam-position monitor. The maximum-likelihood method used has been found to be bias free and insensitive to the specific choice of cut values used, nuclear interactions at the beam pipe, small misalignments of drift chambers, uncertainties in backgrounds, etc. The resulting $c\tau$ is $136 \pm 46^{+18}_{-16}$ μm which corresponds to the lifetime of $(4.6 \pm 1.5^{+0.6}_{-0.5}) \times 10^{-13}$ sec. This is consistent with the world average[1] $(3.9 \pm 0.4) \times 10^{-13}$ sec.

If the semileptonic decays do not depend on the flavor of the spectator quark, the semileptonic decay rate of D^0 should be the same as that of D^+. However, the semileptonic decay rate of D^+ may be larger than that of D^0 by $\sim 10\%$ if the annihilation channel, $c\bar{d} \to e^+\nu +$ gluons, which is Cabibbo-angle suppressed, is not helicity suppressed.[7] This may be checked by comparing the ratio of the lifetimes with the ratio of the semileptonic branching fractions. If the semileptonic decay rate is the same for the two mesons, the two ratios should be equal. Using the world average of the $D^\pm$ lifetime[1] $(8.2^{+1.1}_{-0.9}) \times 10^{-13}$ sec, we obtain $\tau_{D^+}/\tau_{D^0} = 1.8 \pm 0.7$, which is compared with the recent measurement[3] $B(D^+ \to eX)/B(D^0 \to eX) = 2.3^{+0.5+0.1}_{-0.4-0.1}$. Thus, the data are consistent with the same semileptonic decay rates for D^0 and D^+. However, the absence of helicity suppression in the annihilation channel of D^+ in the semileptonic mode is not ruled out.

The standard theory can predict the D^0 semileptonic decay rate as a function of the effective charm-quark mass,[5]

$$\Gamma_{\text{Sl}} = \Gamma_\mu \left[\frac{M_c}{M_\mu} \right]^5 g \gamma_{\text{QCD}} ,$$

where Γ_μ is the muon decay rate, M_c is the effective charm-quark mass, M_μ is the muon mass, g is the phase-space factor, and γ_{QCD} is the QCD correction factor. Small variations in M_c result in large changes in Γ_{Sl}. Thus, a measurement of the semileptonic decay rate can determine the effective quark mass precisely. This value is a measure of the phase space available to the decay, and expected to be larger than the current quark mass, which is estimated[22] to be around 1.2 GeV/c^2, and smaller than the D^0 mass. Our D^0 lifetime, together with the D^0 semileptonic branching fraction[3] of $7.5 \pm 1.1 \pm 0.4\%$, gives a D^0 semileptonic decay rate Γ_{SL} of $(1.6 \pm 0.6) \times 10^{11}$ sec^{-1}. For $g = 0.56 \pm 0.11$ and $\gamma_{\text{QCD}} = 0.85 \pm 0.05$ (Ref. 23), the effective charm-quark mass in a D^0 meson is $M_c = 1.58 \pm 0.12$ GeV/c^2, which is consistent with the typical constituent mass of charm quark, $M_{J/\psi}/2$, but substantially larger than the current mass.

ACKNOWLEDGMENTS

We wish to thank M. Peskin for stimulating discussions. We also acknowledge the contributions to DELCO by the technical staffs of Caltech, SLAC Group A, SLAC Group G, and the PEP Division. A. C. and G. B. thank the French National Scientific Research Center, and E. E. the A. v. Humboldt Foundation. This work was supported in part by the Department of Energy, under Contract numbers DE-AC03-76SF00515 and DE-AC03-81-ER40050, and the National Science Foundation.

---

[a]Present address: CERN, CH-1211, Geneva 23, Switzerland.
[b]Present address: Watkins-Johnson Co., 2525 North First Street, San Jose, CA 95131-1097.
[c]Present address: University of Victoria, Dept. of Physics, P.O. Box 1700, Victoria, B.C., Canada V8W 2Y2.
[d]Present address: DESY, F-22, Notkestrasse 85, D-2000 Hamburg 52, West Germany.
[e]Present address: Department of Physics, Beijing University, Beijing, The People's Republic of China.
[f]Present address: Institute of High Energy Physics, P.O. Box 918, Beijing, The People's Republic of China.
[g]Present address: National Laboratory for High Energy Physics, KEK, Oho-machi, Tsukuba-gun, Ibaraki-ken, 305 Japan.
[h]Present address: Spectra Physics, 3333 North 1st St., San Jose, CA 95134-1995.
[i]Present address: Fakultät für Physik, Albert-Lidwigs-Universität, Hermann-Herder Strasse 3, 7800 Freiburg, West Germany.
[j]Present address: L.A.P.P., Annecy-Le-Vieux, BP 909 France 74019.
[k]Present address: Ford Aerospace, 3939 Fabian Way, Mail Stop G-82, Palo Alto, CA 94303.
[l]Present address: University of Geneva, Dept. of Physics, 32 Boulevard d'Yuoy, 1211 Geneva, Switzerland.
[m]Present address: Hughes Aircraft Co., Mail Station R8-2660, P.O. Box 92426, L.A., CA 90009.
[n]Present address: 18 Mendon Drive, Lattingtown, NY 11560.

[1]See, for example, N. W. Reary, in *Proceedings of the 1983 International Symposium on Lepton and Photon Interactions at High Energies, Ithaca, New York,* edited by D. G. Cassel and D. L. Kreinick (Newman Laboratory of Nuclear Studies, Cornell University, Ithaca, 1983).

[2]W. Bacino *et al.*, Phys. Rev. Lett. **45**, 329 (1980); R. H. Schindler *et al.*, Phys. Rev. D **24**, 78 (1981).

[3]R. M. Baltrusaitis *et al.*, Phys. Rev. Lett. **54**, 1976 (1985).

[4]Among others, a mechanism to enhance the D^0 nonleptonic decay rate is the W-exchange model: M. Bander, D. Silverman, and A. Soni, Phys. Rev. Lett. **44**, 7 (1980); H. Fritzsch and P. Minkowski, Phys. Lett. **90B**, 455 (1980). And a mechanism to suppress the D^+ nonleptonic decays is the final-state interference in the D^+ decay: B. Guberina, S. Nussinov, R. Peccei, and R. Ruckl, *ibid.* **89B**, 111 (1979). Also, see the references in: L-L. Chau, Phys. Rep. **95**, 1 (1983).

[5]N. Cabibbo and L. Maiani, Phys. Lett. **79B**, 109 (1978).

[6]G. Altarelli *et al.*, Nucl. Phys. **B208**, 365 (1982), and the references therein.

[7]U. Baur and H. Fritzsch, Phys. Lett. **109B**, 402 (1982).

[8]J. M. Yelton *et al.*, Phys. Rev. Lett. **52**, 2019 (1984).

[9]For a general description of the DELCO detector, see: Particle Data Group, Lawrence Berkeley Laboratory Report No. LBL-91 Suppl. UC-37, 1983.

[10]The expected horizontal beam sizes are obtained from $\sigma_x{}^2=\beta_x^*\epsilon_{x0}/2$, where β_x^* is the value of the horizontal β function at the interaction region and ϵ_{x0} is the emittance, both calculated from the configuration of the storage ring.

[11]Particle Data Group, Rev. Mod. Phys. **56**, S50 (1984).

[12]The sign of impact parameter for the general hadronic events is defined to be the sign of the z component of $\mathbf{t}\times\mathbf{b}$, where $\mathbf{t}$ is the track direction. Thus, the distribution of b is expected to be symmetric around zero.

[13]The effect may be estimated as follows: If the thrust axis is used as the D^0 direction, the general hadronic tracks have $\langle b \rangle \sim +40\ \mu\text{m}$ (see Sec. III E). When this is added in quadrature to the typical resolution of $\sim 500\ \mu\text{m}$, it increases by only $\sim 0.3\%$.

[14]S. Nussinov, Phys. Rev. Lett. **35**, 1672 (1975).

[15]H. Yamamoto *et al.*, Phys. Rev. Lett. **54**, 522 (1985).

[16]The Monte Carlo method uses the LUND e^+e^- event generator [T. Sjöstrand, Comput. Phys. Commun. **28**, 229 (1983)] and includes detailed simulations of drift-chamber hits and Čerenkov responses. The $c\tau$'s used in the Monte Carlo method are 420 μm for hadrons containing a b quark, 130 μm for D^0, 280 μm for D^+, 60 μm for F^+, and 70 μm for Λ_c. For the strange particles, the values are taken from Particle Data Group, Rev. Mod. Phys. **56**, S12 (1984).

[17]An upper limit on $\Gamma(b\rightarrow ul\nu)/\Gamma(b\rightarrow cl\nu)$ of 4% has been set by A. Chen *et al.*, Phys. Rev. Lett. **52**, 1084 (1984).

[18]N. Lockyer *et al.*, Phys. Rev. Lett. **51**, 1316 (1983); E. Fernandez *et al.*, *ibid.* **51**, 1022 (1983); M. Althoff *et al.*, Phys. Lett. **149B**, 524 (1984).

[19]D. Klem *et al.*, Phys. Rev. Lett. **53**, 1873 (1984).

[20]The large round-off error that occurs when κ is small can be avoided by using the approximation $xe^{x^2}\text{erfc}(x)=0.564\,190-0.274\,030/x^2$ for x^2 greater than ≈ 50. For example, see: M. Abramowitz and I. Stegun, *Handbook of Mathematical Functions* (National Bureau of Standards, Washington, D.C., 1972), p. 316.

[21]Bins with small number of counts have been combined.

[22]For example, see J. Gasser and H. Leutwyler, Phys. Rep. **87**, 77 (1982).

[23]The value and error of g correspond to $M_s/M_c=0.28\pm0.05$. The QCD correction factor γ_{QCD} mainly depends on the value of $\Lambda_{\overline{\text{MS}}}$ ($\overline{\text{MS}}$ is the modified minimal-subtraction scheme), which is taken to be 150 ± 100 MeV. (See, for example, Ref. 5.)